The *full-of-bacteria* gene is required for phagosome maturation during immune defense in *Drosophila*

Mohammed Ali Akbar,[1] Charles Tracy,[1] Walter H.A. Kahr,[3] and Helmut Krämer[1,2]

[1]Department of Neuroscience and [2]Department of Cell Biology, University of Texas Southwestern Medical Center, Dallas, TX 75390
[3]Division of Haematology/Oncology, Program in Cell Biology, Department of Paediatrics, The Hospital for Sick Children, University of Toronto, Toronto, Ontario M5G 1X8, Canada

Arthrogryposis, renal dysfunction, and cholestasis (ARC) syndrome is a fatal recessive disorder caused by mutations in the *VPS33B* or *VPS16B* genes. Both encode homologues of the Vps33p and Vps16p subunits of the HOPS complex necessary for fusions of vacuoles in yeast. Here, we describe a mutation in the *full-of-bacteria* (*fob*) gene, which encodes *Drosophila* Vps16B. Flies null for *fob* are homozygous viable and fertile. They exhibit, however, a defect in their immune defense that renders them hypersensitive to infections with nonpathogenic bacteria. *fob* hemocytes (fly macrophages) engulf bacteria but fail to digest them. Phagosomes undergo early steps of maturation and transition to a Rab7-positive stage, but do not mature to fully acidified phagolysosomes. This reflects a specific requirement of *fob* in the fusion of phagosomes with late endosomes/lysosomes. In contrast, cargo of autophagosomes as well as endosomes exhibit normal lysosomal delivery in *fob* cells. These findings suggest that defects in phagosome maturation may contribute to symptoms of ARC patients including recurring infections.

Introduction

Phagocytosis is an important element of the defense mechanisms against microbial invaders. Microbes are engulfed into early phagosomes by actin-driven extensions of the plasma membrane. Initial properties of phagosomes are dictated by their origination from the plasma membrane, but fusion with endosomes quickly initiates phagosomal maturation (Flannagan et al., 2009). Continued maturation of phagosomes depends on the fusion with early and late endosomal compartments, and eventually lysosomes (Kinchen and Ravichandran, 2008).

As phagosomes mature, they transition through an early stage marked by the presence of the GTPase Rab5 and its effectors (Kinchen and Ravichandran, 2008). Among them, Mon1/SAND-1 proteins aid in the conversion from Rab5- to Rab7-positive late phagosomes (Kinchen and Ravichandran, 2010), which is equivalent to their role in endosome maturation (Poteryaev et al., 2010). Rab7, subsequently, is required for phagosomes and late endosomes to fuse with lysosomes (Bucci et al., 2000; Harrison et al., 2003).

HOPS (homotypic fusion and vacuole protein sorting) is a multiprotein complex that originally was characterized in yeast for its role in vacuolar fusions (Sato et al., 2000; Seals et al., 2000). The HOPS complex acts as a tethering factor, stimulates Rab nucleotide exchange, and coordinates the interaction of SNAREs during lysosomal fusions (Nickerson et al., 2009; Wickner, 2010). In multicellular organisms, HOPS complex function is necessary for the biogenesis of lysosomes and lysosome-related organelles (Rojo et al., 2001; Sadler et al., 2005; Maldonado et al., 2006). In *Drosophila*, homologues of the HOPS subunits Vps18p and Vps33p are encoded by *deep orange* and *carnation*. Both genes are named for their role in the biogenesis of pigment granules in the fly eye, and, together with *Vps16A*, they are required for lysosomal delivery of cargo from endosomes and autophagosomes (Sevrioukov et al., 1999; Sriram et al., 2003; Pulipparacharuvil et al., 2005; Lindmo et al., 2006; Akbar et al., 2009). Similarly in mice, the *buff* mutation, because of a missense mutation in the VPS33A gene, causes abnormal pigmentation (Suzuki et al., 2003) and progressive neurodegeneration, presumably because of a defect in lysosomal delivery (Chintala et al., 2009). Furthermore, an RNAi screen in *Caenorhabditis elegans*

Correspondence to Helmut Krämer: hkrame@mednet.swmed.edu

Abbreviations used in this paper: AMP, antimicrobial peptide; ARC, arthrogryposis, renal dysfunction, and cholestasis; Avl, Avalanche; *fob*, *full-of-bacteria*; qRT-PCR, quantitative RT-PCR.

Supplemental material can be found at:
http://doi.org/10.1083/jcb.201008119

The Rockefeller University Press $30.00
J. Cell Biol. Vol. 192 No. 3 383–390
www.jcb.org/cgi/doi/10.1083/jcb.201008119

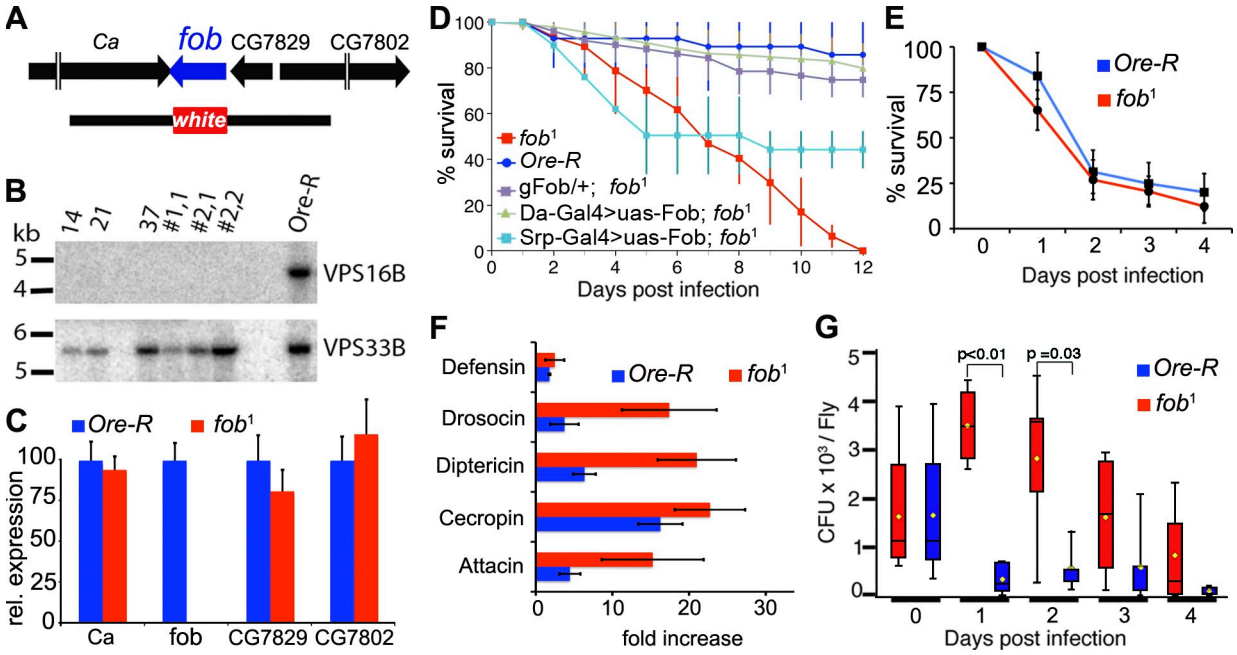

Figure 1. **A *fob* null allele is hypersensitive to infections with *E. coli*.** (A) Schematic representation of the *Drosophila fob* gene and its neighbors. The targeting fragment generated in vivo (Gong and Golic, 2003) contains portions of neighboring genes around the mini-*white* gene (red box). (B) Southern hybridization with the entire *fob* gene yielded a signal with Ore-R (wt) but with any *fob* allele. Reprobing the same membrane with dVps33b confirmed the presence of DNA in all lanes. (C) qRT-PCR showed no expression of *fob* but similar levels of expression for neighboring genes in fob^1 compared with wild type. Gene expression levels were normalized with rp49 as an internal control and are shown relative to wild type. (D and E) Survival after infection was measured for wt, fob^1, and rescued fob^1 flies after injection with *E. coli* (D) or *E. faecalis* (E). (F) Induction of AMP genes 6 h after injection with *E. coli* (Drosocin, Diptericin, Cecropin, and Attacin) or 12 h after injection with *E. faecalis* (Defensin). (G) Bacterial load in injected flies at the indicated day after injection with *E. coli*. Error bars indicate standard deviation.

has implicated HOPS subunits in phagosomal maturation (Kinchen et al., 2008).

Metazoan genomes encode two Vps33p homologues (Pevsner et al., 1996). In *Drosophila*, their functions are distinct, as none of the *car/Vps33A* phenotypes can be rescued by Vps33B expression (Akbar et al., 2009). A role for Vps33B in the clearance of *Mycobacterium tuberculosis* bacteria was revealed by the identification of Vps33B as a target of the bacterial virulence factor PtbA, a phosphatase critical for the intracellular persistence of these microbes (Bach et al., 2008). Importantly, mutations in Vps33B cause a fatal recessive disorder named arthrogryposis, renal dysfunction, and cholestasis (ARC) syndrome (Gissen et al., 2004). Cells from ARC patients exhibit diverse defects including mislocalization of a subset of apical proteins (Gissen et al., 2004) and defects in the biogenesis of platelet α-granules (Lo et al., 2005), but the underlying trafficking defects are not well understood. An important aspect of Vps33B function is its binding to Vps16B, an interaction that is conserved from invertebrates to humans (Pulipparacharuvil et al., 2005; Zhu et al., 2009; Cullinane et al., 2010). Relevance of this interaction was confirmed by the discovery of mutations in VPS16B as the second major cause of ARC syndrome (Cullinane et al., 2010).

Here, we describe a mutation in the *full-of-bacteria* (*fob*) gene, which encodes *Drosophila* Vps16B. To our surprise, flies null for *fob* were homozygous viable and fertile. They exhibit, however, a profound defect in phagosome maturation, and as a consequence are sensitive to infections with normally nonpathogenic microbes. These findings suggest that defects in phagosome maturation may contribute to symptoms of ARC patients, including their recurring infections (Gissen et al., 2006; Hershkovitz et al., 2008; Jang et al., 2009).

Results and discussion

Fob is required for normal immune defense

A fob^1 null allele (Fig. 1, A and B) was generated by ends-out homologous recombination (Gong and Golic, 2003). fob^1 flies were null for *fob* expression but had no change in the transcription of neighboring genes (Fig. 1 C). Homozygous fob^1 and hemizygote (fob^1/Df(3R)BSC547) flies were viable, fertile, and displayed no morphological defects.

ARC patients present with recurrent infections at a high frequency (Gissen et al., 2006; Hershkovitz et al., 2008; Jang et al., 2009), thus we wondered whether microbial infections also threaten fob^1 flies. We compared the survival of fob^1 and wild-type flies upon injections with bacteria. Interestingly, fob^1 mutants were strongly susceptible to infections with *Escherichia coli*, bacteria that are nonpathogenic to wild-type flies (Fig. 1 D, $P < 0.0001$ logrank). Survival of fob^1 flies was significantly improved by expression of fob cDNA in hemocytes (Srp-Gal4 compared with fob^1, $P = 0.005$ logrank); its ubiquitous expression or a genomic rescue construct further improved survival to wild-type levels (Da-Gal4, $P = 0.5$; gFob, $P = 0.3$; both logrank vs. Ore-R). Pathogenic *Enterococcus faecalis* microbes killed fob^1 flies only slightly faster than wild type

(Fig. 1 E, P = 0.005 logrank). Survival of flies after microbial infections depends, in part, on the induction of antimicrobial peptides (AMPs) through the activation of the IMD or Toll pathways (Hoffmann, 2003). Therefore, we compared AMP gene expression in infected *fob*[1] and wild-type flies relative to their counterparts injected with PBS only. Quantitative RT-PCR (qRT-PCR) showed that infected *fob*[1] flies induced AMP expression, which indicates that IMD or Toll signaling was not inhibited (Fig. 1 F). Given their ability to mount an AMP response against gram-positive and gram-negative bacteria, *fob*[1] must be lacking in a different aspect of the host defense.

Early steps in phagocytosis do not require Fob

Another facet of host defense is the phagocytosis of invading microbes. After injection with pHrodo-labeled bacteria into their abdomen, wild-type flies displayed a characteristic accumulation of fluorescence in sessile hemocytes in the thorax (Fig. 2 A). This reflects the uptake of bacteria into hemocyte phagosomes and their subsequent acidification (Cuttell et al., 2008). In comparison, *fob*[1] flies exhibited weaker fluorescence, but the number of immobilized bacteria did not seem drastically reduced, which is consistent with the presence of active phagocytic sessile hemocytes. In contrast, in *eater* flies, the number of bacteria appeared reduced but the signal strength of individual punctae was similar to wild type (Fig. 2 A). The loss of one of several phagocytic receptors in *eater* flies reduces phagocytic uptake but not phagosome maturation and acidification (Kocks et al., 2005). In contrast, the reduced pHrodo fluorescence in *fob*[1] flies suggested a defect in phagosomes acidification.

To address this issue at higher resolution, we analyzed phagocytosis in primary hemocytes from third instar larvae (Pearson et al., 2003). Compared with wild type, *fob*[1] hemocytes did not exhibit a defect in initial phagocytic uptake of bacteria (Fig. 2, B and C). Subsequently, wild-type cells efficiently digested bacteria (Fig. 2 D), and after a 45-min chase contained only 4.8 ± 3 bacteria (n = 6). In contrast, at this time point, *fob*[1] cells (Fig. 2 E) were still full of bacteria (26 ± 16, n = 6, P < 0.0001). Similarly, elevated levels of bacteria were observed after knockdown of Vps33B or Vps16A (Fig. 2 F). Inability to digest bacteria was also observed in vivo after injection with *E. coli*. In *fob*[1] flies, the bacterial burden remained elevated (Fig. 1 G), as opposed to the efficient clearance of the majority of bacteria in wild-type flies after just 1 d. Together, these data suggest that the poor survival of *fob*[1] flies after injections with nonpathogenic *E. coli* reflects a defect in phagosome maturation.

Phagosome maturation requires Fob

A necessary step in the acquisition of the full degradative potential of phagosomes is their acidification, which can be monitored by imaging the fluorescence ratio of Oregon green/Texas red doubly labeled phagocytosed bacteria. After a 30–45-min chase in wild-type hemocytes, the majority of internalized bacteria appeared degraded as judged by the diffuse appearance of remaining fluorescence, but the few phagosomes that still contained well-defined bacteria had acidified to a mean pH of 5.5 ± 0.15 compared with a mean starting pH of 6.5 ± 0.15

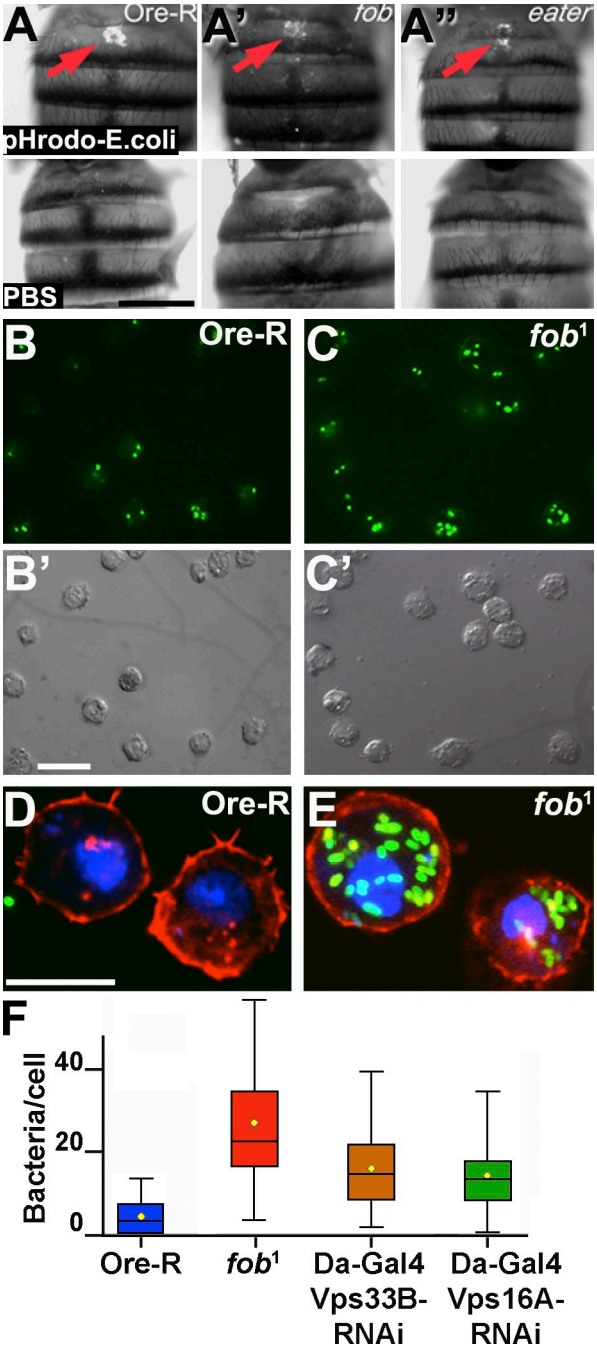

Figure 2. ***fob* mutants exhibit a defect in bacterial clearance.** (A) 2 h after injection, pHrodo-labeled *E. coli* (arrows) were visible around the dorsal vessel in the thorax of wild-type and *eater* flies (Df(3R)D605/Df(3R)Tl-l). In contrast, diffuse weaker signals appeared in *fob*[1] flies. (B) Hemocytes were allowed to engulf FITC-labeled *E. coli* for 15 min, and, after quenching fluorescence of external bacteria with Trypan blue, the fluorescence of phagocytosed bacteria was visible in wild-type (B) and *fob*[1] (C) cells visualized by differential interference contrast microscopy (B′ and C′). (D and E) After 45 min of chase, bacteria were cleared from wild type (D) but accumulated inside *fob*[1] hemocytes (E). (F) Box and whisker plots display the number of bacteria detected in hemocytes of indicated genotypes after 45 min of chase. Bars: (A) 0.5 mm; (B and C) 25 µm; (D and E) 10 µm.

(Fig. 3 A and Fig. S1). In contrast, *fob*[1] phagosomes acidified only minimally, if at all: the starting mean pH of 6.6 ± 0.12 was only lowered to pH 6.3 ± 0.13 after a 30-min chase (Fig. 3 B). In accordance with this finding, electron microscopy of isolated

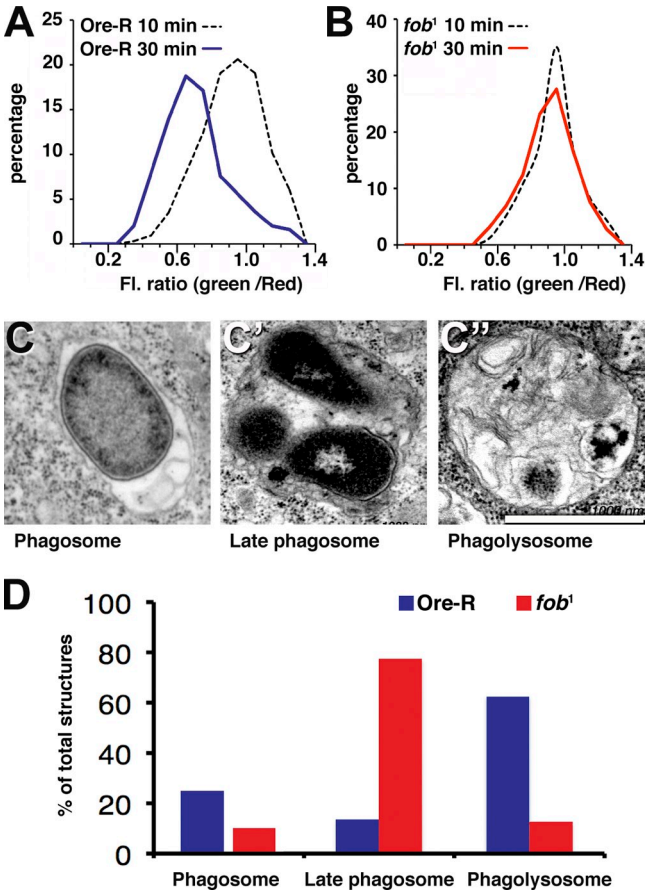

Figure 3. ***fob* phagosomes fail to mature.** Double-labeled bacteria were allowed to internalize for 10 min (broken line) or 30 min (solid line), and images were captured for 15 min. The distribution of fluorescence ratios is shown for Ore-R (A) and *fob*[1] (B). The fluorescence ratio relates to pH as shown in Fig. S1. (C) Electron micrographs of phagosomes detected after a 30-min chase of phagocytosed *E. coli*. Phagosomal structures were broadly classified in three categories based on their ultrastructural appearance: phagosome (C), late phagosome (C′) and phagolysosomes (C″). Bar, 1 µm. (D) Relative distribution of different categories of phagosomes in Ore-R and fob1. Data were collected from two independent sets of experiments with equivalent results. Quantification was performed in triplicate with a representative example shown in D.

fob[1] hemocytes revealed that after a 30-min chase, phagocytosed bacteria were predominantly present in late phagosomes (Fig. 3, C and D) that were characterized by a mix of undigested or mildly degraded bacteria (Fig. 3 C′). In contrast, after a 30-min chase in wild-type hemocytes, the majority of bacteria had reached phagolysosomes (Fig. 3, C″ and D) characterized by strongly degraded content (Fig. 3 C″).

Phagosomes mature by interacting with endosomal compartments (Desjardins et al., 1994). Thus, we explored endosomal markers, including Rab GTPases (Smith et al., 2007), as indicators of phagosome maturation. We found that a Rab-5 effector, Rabenosyn-5 (Rbsn-5), was present on *fob*[1] and wild-type phagosomes (Fig. 4, A and F). Rbsn-5 is a FYVE domain protein whose phagosomal localization depends on activation of phosphatidylinositol 3-kinases (PI3K) and Rab5 (Stenmark et al., 1995; Vieira et al., 2003). These data indicated that early steps in phagosome maturation, including the generation of 3-phosphoinositides and subsequent recruitment of Rab5 effectors, are normal in *fob*[1] mutant phagosomes. This conclusion was further supported by the presence of Avalanche (Avl), an early endosomal SNARE (Lu and Bilder, 2005), on Rbsn-5–positive phagosomes in *fob*[1] and wild-type hemocytes (Fig. 4, A and F). This indicates that *fob*[1] mutants have normal early endosome–phagosome fusion.

A subsequent step in phagosome maturation involves the exchange of Rab5 to Rab7, similar to their exchange observed in endosomes (Vieira et al., 2002; Rink et al., 2005). 62 ± 26% of phagosomes in *fob*[1] hemocytes were decorated by Rab7 compared with 36 ± 14% in wild type, which indicates that Rab5-to-Rab7 conversion was not inhibited in *fob*[1] (Fig. 4, B, B′, and F). This significantly increased presence of Rab7 on phagosomes in *fob*[1] cells ($P < 0.0001$) suggests that phagosomes are stalled at this stage. This is reminiscent of the dramatic increase of Rab7 on late endosomes in *car*-null cells (Fig. S2 K; Akbar et al., 2009) and is consistent with Rab7 recruitment not being sufficient to induce fusion with lysosomes (Vieira et al., 2003). We explored other markers and found that Hook was present on 31 ± 8% of wild type but only on 6 ± 2% of *fob*[1] phagosomes, without ever decorating entire phagosomes as we observed in wild-type cells (Fig. 4 C). Interestingly, *Drosophila* Hook has been implicated in the maturation of multivesicular bodies (Sunio et al., 1999), which are involved in phagosome maturation (Philips et al., 2008). Considering the connection between endosomal and phagosomal maturation pathways, our data suggest that *fob*[1] phagosomes failed to acquire late endosomal/lysosomal characteristics due a loss of fusion with those compartments.

Fob mutants exhibit a specific defect in the fusion of lysosomes with phagosomes

Several lines of evidence argue that the *fob*[1] phagosomal maturation defect does not reflect a block in endocytic trafficking. For example, distribution of Boss and Delta ligands, which sensitively respond to loss of Vps16A or Car/Vps33A function (Fig. S2, I and J; Pulipparacharuvil et al., 2005; Akbar et al., 2009), was not altered in eye discs from *fob*[1] larvae, indicating that endocytic trafficking proceeded normally (Fig. S2, C–H). Furthermore, eyes of 2-d-old flies exhibited normal ommatidial organization (Fig. S2, A and B), which indicates that *fob*[1] mutants have no significant defects in Notch or EGF receptor signaling. The recurrent use of these signaling pathways during eye development provides a sensitive read-out for defects in formation of apical polarity, adherens junctions, or changes in endocytosis, lysosomal delivery, or recycling. Furthermore, starvation-induced autophagy, which requires fusion with lysosomes, is also normal in *fob*[1] larvae (Fig. S2, L–O). Together, these data indicate that *fob* is not essential for endocytic or autophagic routes engaged during developmental signaling or cell remodeling and instead point to a specific requirement of *fob* for the fusion of phagosomes to lysosomes.

To directly test this hypothesis, we functionally labeled lysosomes by allowing hemocytes to internalize dextrans by fluid phase endocytosis. After a 90-min chase in wild-type cells, 60–80% of dextran had reached lysosomes, as measured by their colocalization with LysoTracker (Fig. 4 D). This was not

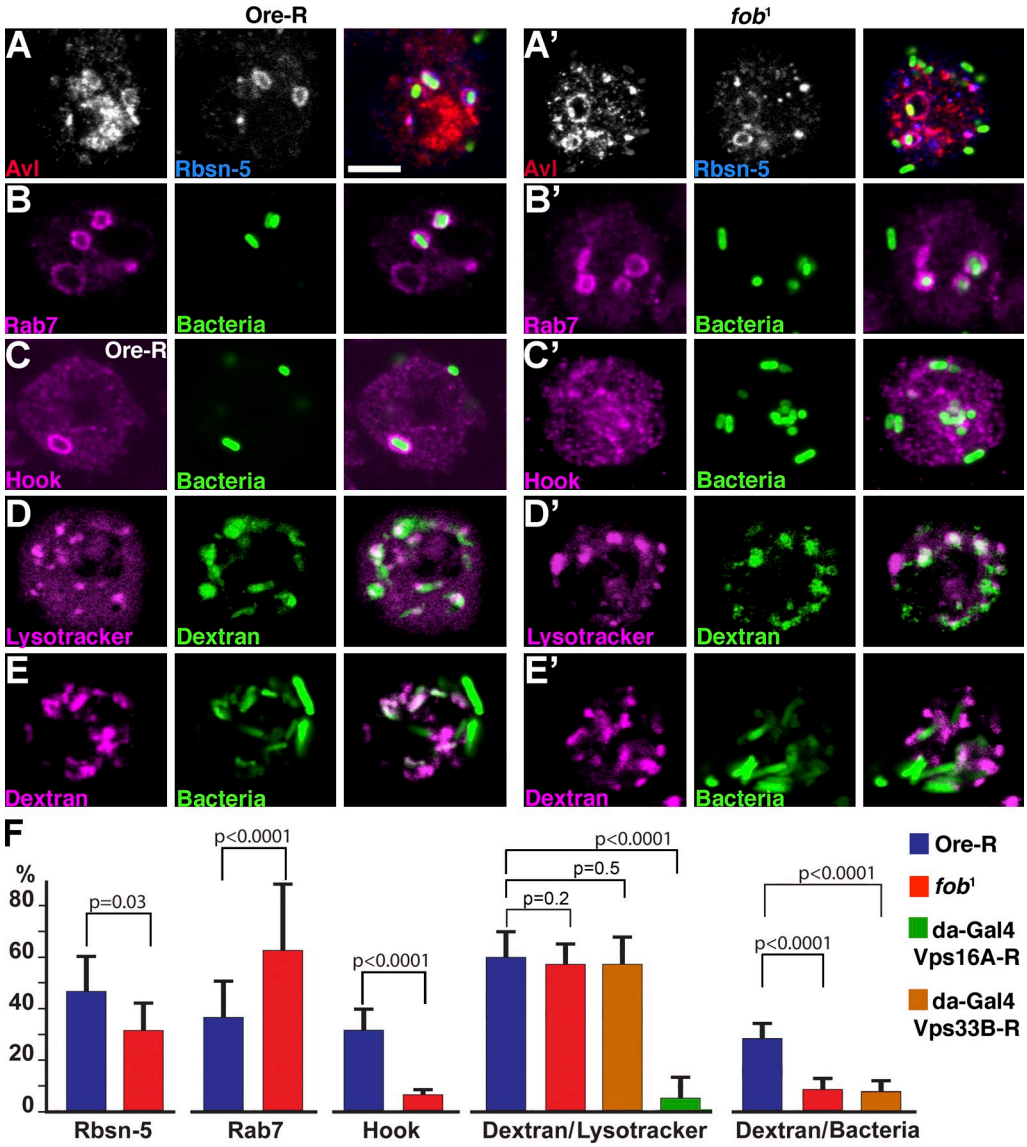

Figure 4. ***fob* is required for the fusion of phagosomes with lysosomes.** Micrographs show hemocytes isolated from wild-type (A–E) or *fob*^{1} (A′–E′) larvae. (A–C) Hemocytes were allowed to phagocytose FITC-labeled *E. coli*, and were immunostained for Avl (red) and Rbsn-5 (blue; A), Rab7 (B), or Hook (C). (D) Hemocytes were allowed to internalize dextran–Alexa Fluor 488 (10 kD), which after a 90-min chase partially colocalized with LysoTracker in wild type (D) and *fob*^{1} (D′), indicating functional labeling of lysosomes by dextran. (E) Hemocytes with lysosomes preloaded with internalized Texas red–dextran were allowed to phagocytose GFP-labeled *E. coli*. After 30–45 min of chase, the bacteria colocalized with dextran in wild-type (E) but not *fob*^{1} hemocytes (E′). For display, images were imported into Photoshop (Adobe) and adjusted for gain, contrast, and gamma settings. Bar, 5 µm. (F) Bar graphs indicate percentages of bacteria in phagosomes positive for the indicated markers or the percentage of dextran in LysoTracker-positive structures (error bars indicate standard deviation). Hemocytes were harvested from larvae with indicated genotypes.

significantly altered in *fob*^{1} or Vps33B knockdown hemocytes, which is consistent with the notion that neither is necessary for endocytic trafficking. In contrast, in Vps16A knockdown hemocytes, dextran failed to reach lysosomes (Fig. 4 F), which suggests that lysosomal dysfunction (Pulipparacharuvil et al., 2005) rather than a defect in phagocytosis may be the primary cause of reduced bacterial clearance in Vps16A knockdown hemocytes (Fig. 2 F). Next, hemocytes containing dextran-prelabeled lysosomes were allowed to phagocytose bacteria. After a 30–45-min chase, 28 ± 7% of bacteria-containing phagosomes in wild-type hemocytes colocalized with pre-endocytosed dextran, which is consistent with their fusion with lysosomes (Fig. 4 E). In contrast, only few 8.6 ± 4% *fob*^{1} or 7.6 ± 5% Vps33B-knockdown phagosomes colocalized with dextran, which indicates their failure to fuse with the prelabeled lysosomes. Because the evaluation of late-stage bacterial phagosomes is complicated by the continuous degradation of bacteria, we also tested the phagocytosis of latex beads. Here the loss of phagosome/lysosome fusion was even more evident, as after a 30–45-min chase, 50 ± 13% of latex beads colocalized with dextran in wild type, but only 8 ± 2% colocalized in *fob*^{1} hemocytes.

Vps16B proteins in various species tightly interact with the corresponding Vps33B partners (Fig. S3 A; Pulipparacharuvil et al., 2005; Zhu et al., 2009; Cullinane et al., 2010). Consistent with a shared role of this complex in phagocytosis, dVps33B knockdown also rendered flies hypersensitive to *E. coli*

(Fig. S3 C), as we observed in *fob*^{1} mutants. Previous analyses of these complexes focused on possible functions in endosomes (Gissen et al., 2004; Matthews et al., 2005; Zhu et al., 2009; Cullinane et al., 2010). Surprisingly, we did not detect any requirement of *fob* in endocytic trafficking in *Drosophila*. This is distinct from our findings for its paralogue dVps16A, which together with Carnation and Deep orange is required for lysosomal delivery of endocytic and autophagic cargo and for biogenesis of pigment granules (Fig. 4 F and Fig. S2, I–K; Pulipparacharuvil et al., 2005; Akbar et al., 2009). Instead, we found that *fob* is specifically required for fusion of phagosomes with late endosomes/lysosomes. This specificity distinguishes *fob* from other genes, such as *rab7* or genes encoding ESCRT subunits, which are required for phagosome maturation but also participate in endocytic delivery to lysosomes (Philips et al., 2008). Together, these data indicate that Vps16A and Vps16B, and their corresponding binding partners Vps33A and Vps33B, have nonredundant functions in these pathways (Suzuki et al., 2003; Lo et al., 2005; Pulipparacharuvil et al., 2005; Akbar et al., 2009).

A possible role of Vps16B and Vps33B proteins in phagocytosis is also consistent with several previous observations. Dephosphorylation of Vps33B is one among several strategies that *M. tuberculosis* bacteria use to inhibit phagosome maturation and thereby escape their degradation (Bach et al., 2008). The recurrent bacterial sepsis common among patients with ARC syndrome (Gissen et al., 2006) may reflect deficiencies of phagocytic cells in clearing infections. Similarly, macrophage-like coelomocytes are among the cell types strongly affected in mutants for *spe-39*, which encodes the *C. elegans* homologue of Vps16B (Zhu et al., 2009), and other HOPS subunits have been implicated in phagosome/lysosome fusion as well (Kinchen and Ravichandran, 2010). Together, these data point to the possibility that phagosome–lysosome fusion may be the ancestral function of Vps16B/Vps33B proteins, and it will be important to identify which aspects of ARC syndrome are caused by defects in phagocytosis.

Materials and methods

Fly genetics and generation of *fob*^{1} mutant

Ends-out homologous recombination was used for generating a *fob*-null allele (Gong and Golic, 2003). Stepwise, left (5,906 bp) and right (5,293 bp) flanking regions of the *fob* gene were cloned into p[w25.2] vector yielding pw25-16Bko. Primers for amplification of left and right regions were: left, 5′-ATTTGCGGCCGCTGCGTGGTGAGTTTGCAC-3′ and 5′-ATTTGCGGCCGCGCTCAAGTTGTAAAATTGACTTTCT-3′, and right, 5′-TTGGCGCGCCGCACAGACATGGTCGCACTA-3′ and 5′-AACGTAC-GATCACGGCCAGTTACTCCAC-3′. A transgenic line carrying this donor on the second chromosome was selected for targeting (Gong and Golic, 2003). Candidates for which the mini-*white* gene of pw25-16Bko mapped to the third chromosome were analyzed by probing Southern blots, first with the entire *fob* gene and then with *dVps33B* to control for loading.

For infections and immunohistology, the following lines were used: Oregon-R (wt), *fob*^{1}, w^{1118}; *fob*^{1}/Df(3R)BSC547/TM6C, Sb1, *eater* trans heterozygous [Df(3R)D605/Df(3R)TI-I], da-Gal4/uas-Vps33B-RNAi, and da-Gal4/Vps16A-RNAi (Pulipparacharuvil et al., 2005). Clones for *car*-null cells were generated in the eye discs, which were stained as described previously (Akbar et al., 2009). Gal4 drivers and deficiencies were obtained from the Bloomington Stock Center.

For rescue experiments, the fob coding unit was amplified using the primer set 5′-CCGCTCGAGATGGAGGAGCAGAAGCTGAT-3′ and 5′-GGGGTACCTTACAACTTGAGCTTGATGTTGTCC-3′. The unit was then cloned into the pUASt vector using XhoI and Acc65I, and the resulting uas-Myc-Fob transgene was expressed under control of Da-Gal4 or Srp-Gal4 in *fob*^{1} background. Alternatively, a genomic fragment containing sequences 1.8 kb upstream and 0.8 kb of downstream of the fob coding region was cloned into a derivative of pCaSp4 for the generation of a transgenic line. For Vps33B-RNAi experiments, a 381-bp inverted repeat (bp 1,180–1,561 of the Vps33B mRNA; available from GenBank/EMBL/DDBJ under accession no. NM_143138.1) was clone into a modified pWIZ vector (Pulipparacharuvil et al., 2005) and expressed in transgenic flies under uas/Gal4 control. Plasmids containing the fob, vps33B, and Car cDNAs templates had been generated by the Berkeley Drosophila Genome Project and were obtained from the Drosophila Genomics Resource Center.

Infection experiments

E. coli (DH5α, amp resistance, GFP) and *E. faecalis* cultures were grown overnight in Luria Bertani (LB) or brain heart infusion medium (BHI) medium at 37°C. Female virgin flies (5 d old) were injected (Schneider et al., 2007) with 80 nl PBS containing a mean of 1,600 *E. coli* (OD_{600} = 0.1) or 200 *E. faecalis* (OD_{600} = 0.005). Sterile PBS was injected as a control. Injected flies (20 flies per vial) were reared at 25°C, 65% humidity, on yeast-agar-molasses food. Injections were performed with a pico-injector (model PLI-188; Nikon) fitted with glass capillary needles. Injections were performed in triplicate (total of 60 flies) for each group with either of the indicated microbes and PBS control on the same day. All injection experiments were repeated 8–10 times. For each survival curve, flies were counted every 24 h, and bars represent mean values with standard deviation. Data were analyzed using the SAS software (SAS Institute, Inc).

To determine bacterial load, flies were injected with *E. coli* (DH5α, kanamycin resistant, five flies per data point) and homogenized after the indicated time (Schneider et al., 2007). Serial dilutions were plated and colonies were counted for each time point. Data are plotted as boxes with whiskers. The mean is indicated with a diamond. The boxes indicate 25th and 75th percentiles; the bold line is the 50th percentile, whereas the whiskers show the complete range of the data.

pHrodo-*E. coli* bioparticles (Invitrogen) were suspended according to manufacturer's instructions, and 80 nl were injected. After 2 h, flies were mounted and imaged on a microscope with 1.5× magnification (SZX12; Olympus). During imaging, exposure parameters were set such that for Oregon-R the brightest spots were not saturated. FITC-*E. coli* (catalogue No. F6694; Invitrogen) were used for phagocytosis and immunostaining experiments in hemocytes.

For qRT-PCR experiments, RNA was isolated using TRIzol (Invitrogen) according to the manufacturer's instructions. For anti-microbial peptide measurements, RNA was isolated from five flies after injection (6 h for *E. coli* and 12 h for *E. faecalis*). qRT-PCR was performed using a DNA-free, high-capacity cDNA reverse transcription kit (Fast SYBR Green master mix; Applied Biosystems) and a Fast Real-Time PCR System (7500; Applied Biosystems). Each data point was repeated three times beginning from injection. Values were normalized first with rp49 as an internal control and then expressed as fold change compared with flies injected with PBS as control. The following primer sets were used for amplification: fob left, 5′-TATTGGAACC-GATCCTCTCG-3′; fob right, 5′-CACCAGTTTCAATGCCTCCT-3′; Ca left, 5′-CCATATCAGCCGCATTTCTT-3′; Ca right, 5′-AAGCTGGCATCGTTCT-GACT-3′; CG7829 left, 5′-CAGGAACCTACTGGGCAAAA-3′; CG7829 right, 5′-AGTAGACTCCCGGCTTGTCC-3′; CG7802 left, 5′-GTCGCGA-CATCGACACTTC-3′; CG7802 right, 5′-CGTTGGCAGTGAATGTGGT-3′; Attacin A left, 5′-TGCAGAACACAAGCATCCTAA-3′; Attacin A right, 5′-TAAGGAACCTCCGAGCACCT-3′; Cecropin A1 left, 5′-TCTTCGTTTTC-GTCGCTCTC-3′; Cecropin A1 right, 5′-ACATTGGCGGCTTGTTGAG-3′; Defensin left, 5′-GATGTGGATCCAATTCCAGA-3′; Defensin right, 5′-CTT-TGAACCCCTTGGCAAT-3′; Diptericin left, 5′-ACCGCAGTACCCACTCA-ATC-3′; Diptericin right, 5′-CCATATGGTCCTCCCAAGT-3′; G Drosocin left, 5′-TTCACCATCGTTTTCCTGCT-3′; Drosocin right, 5′-GGCAGCTTGAGTCAG-GTGAT-3′; Drosomycin left, 5′-GTACTTGTTCGCCCTCTTCG-3′; Drosomycin right, 5′-ACTGGAGCGTCCCTCCTC-3′; rp49 left, 5′-ATCGGTTACGGATC-GAACAA-3′; and rp49 right, 5′-GACAATCTCCTTGCGCTTCT-3′.

Hemocyte isolation and phagocytosis experiments

Hemocytes were collected from 60–80 wandering third instar larvae in Schneider's *Drosophila* medium (10% heat-inactivated FBS) containing glass-bottom culture dishes. Cells were allowed to settle down for 15 min and washed with Schneider's media followed by incubation with the indicated bacteria or dextran.

After a 15-min incubation at 4°C, unbound bacteria were washed out and phagocytosed bacteria were chased for the various times. (a) 15 min to measure initial uptake, after which extracellular fluorescent bacteria were quenched with Trypan blue. (b) To visualize late stage phagosomes in life cells, we chased for 30 min, after which we collected images for 15 min. We call this a "30–45 min chase." (c) To capture early or late stage phagosomes by immunofluorescence staining, we fixed after 15–25 min or 30–45 min of chase. (d) We chased for 45 min to analyze bacterial persistence in cells, as at that time most bacteria were digested in wild-type hemocytes. Subsequently, cells were fixed (4% PFA) and counterstained with Phalloidin–Alexa Fluor 546 (Invitrogen). Oregon-R was used as control in all assays. (e) For electron microscopy analysis of phagosome maturation, we chased for 30 min. Cells were fixed with a mixture of 1.5% glutaraldehyde and 2.5% PFA for 2 h, then stained with osmium tetroxide, dehydrated, and embedded in epon. Sections (60–70 nm) were stained with uranyl acetate, dried, and viewed under a transmission electron microscope (120kV; Technai G2 spirit; FEI) with an 11-megapixel Morada camera (Olympus). Data were collected from two independent sets of experiments with equivalent results. Quantification was performed in triplicate, with a representative example shown in Fig. 3 D.

For phagocytosis experiments, *n* refers to the number of independent experiments that were quantified.

pH measurement

To measure acidity (pH), heat-killed *E. coli* (DH5α) were colabeled with the pH-sensitive fluorophore Oregon green 488 and the pH-insensitive carboxy-tetramethylrhodamine (Vergne et al., 1998). To calibrate their pH-dependent fluorescence, bacteria were suspended in phosphate-citrate buffer, pH 2.5–7.0, and imaged using a 63×, NA 1.4 lens on a confocal microscope (LSM510; Carl Zeiss, Inc.). Fluorescence ratios were determined for individual bacteria using ImageJ. To measure changes in phagosome pH, *fob*[1] or wild-type hemocytes were incubated with double-labeled bacteria (2–4 × 10^7 ml^{-1}) at 4°C for 15 min. After a 10-min or 30-min chase, fluorescence ratios were measured from intact bacteria that did not appear degraded as indicated by diffuse fluorescence.

Immunofluorescence and dextran internalization

Hemocytes were incubated with dextran–Alexa Fluor 488 or dextran–Alexa Fluor 594 (10 kD, 1 mg/ml) for 5 min in PBS, pH 7.4, for monitoring fluid phase endocytosis. Free dextran was removed by washing extensively, and cells were chased for 90 min in Schneider's *Drosophila* medium with 10% heat-inactivated FBS. After that chase, cells were either incubated with LysoTracker (GFP-certified Lyso-ID red lysosomal detection kit; Enzo Biochem, Inc.) or allowed to phagocytose GFP-tagged *E. coli* or latex beads to measure fusion of lysosome to phagosome.

For immunofluorescence staining after phagocytosis, hemocytes were fixed with 4% PFA for 45 min, then washed with PBS with 0.3% saponin. Samples were stained with the indicated primary antibodies rabbit anti-Hook (1:250; Sunio et al., 1999), rabbit anti-Avl (1:1,000; Pulipparacharuvil et al., 2005), rabbit anti–Rbsn-5 (1:5,000; a gift from A. Nakamura; Institute of Physical and Chemical Research Center for Developmental Biology, Kobe, Japan; Tanaka and Nakamura, 2008), rabbit anti-Rab7 (1:3,000; a gift of P. Dolph; Dartmouth College, Hanover, NH; Chinchore et al., 2009); and secondary antibodies labelled with Alexa Fluor 568 and Alexa Fluor 647 and mounted in Vectashield (Vector Laboratories).

Fluorescence images were captured with a 63×, NA 1.4 lens on an inverted confocal microscope (LSM510 Meta; Carl Zeiss, Inc.) at room temperature (21°C). All digital images were imported into Photoshop (Adobe) and adjusted for gain, contrast, and gamma settings.

Statistics

The LIFETEST procedure of SAS 9.2 (SAS Institute Inc.) was used to analyze survival curves by the Kaplan-Meier method. Logrank comparisons were used to assess significance of differences between curves. Student's *t* tests (two-tailed) were used to determine the statistical significance of differences between colony-forming unit counts and changes of Avl/Rbsn-5, Rab7, and Hook localization to phagosomes was identified by bacterial content. At least 50 cells with phagosome structures containing bacteria were used for each of the quantifications. Phagosomes in >100 cells were used for the quantification of dextran/LysoTracker or dextran/bacteria.

Online supplemental material

Fig. S1 shows an in vitro calibration curve for the ratiometric signal from Oregon green/Rhodamine-labeled bacteria with different pH values. Fig. S2 shows the lack of changes in endosomal trafficking or autophagosome maturation in *fob* mutant cells and compares it to the reduced lysosomal delivery after loss of Vps16A or Carnation function. Fig. S3 shows in vivo binding of Fob and Vps33B and the reduced survival of *E. coli*–injected flies after Vps33b knockdown. Online supplemental material is available at http://www.jcb.org/cgi/content/full/jcb.201008119/DC1.

We thank Drs. David Schneider and John Abrams for critical reading of the manuscript and Drs. Akira Nakamura and Patrick Dolph for antibodies. We are grateful to Sanchali Ray for technical assistance. We would like to thank the Bloomington Stock Center for fly stocks, the Berkeley Drosophila Genome Project for producing DNA clones, the Drosophila Genomics Resource Center for their distribution, and the Developmental Studies Hybridoma Bank at the University of Iowa for antibodies. FlyBase provided important information used in this work.

This work was supported by grants from the Canadian Institutes of Health Research (CIHR; MOP-81208) to W.H.A. Kahr, the National Institutes of Health (EY10199) to H. Krämer, and the core grant EY020799.

Submitted: 20 August 2010
Accepted: 2 January 2011

References

Akbar, M.A., S. Ray, and H. Krämer. 2009. The SM protein Car/Vps33A regulates SNARE-mediated trafficking to lysosomes and lysosome-related organelles. *Mol. Biol. Cell.* 20:1705–1714. doi:10.1091/mbc.E08-03-0282

Bach, H., K.G. Papavinasasundaram, D. Wong, Z. Hmama, and Y. Av-Gay. 2008. *Mycobacterium tuberculosis* virulence is mediated by PtpA dephosphorylation of human vacuolar protein sorting 33B. *Cell Host Microbe.* 3:316–322. doi:10.1016/j.chom.2008.03.008

Bucci, C., P. Thomsen, P. Nicoziani, J. McCarthy, and B. van Deurs. 2000. Rab7: a key to lysosome biogenesis. *Mol. Biol. Cell.* 11:467–480.

Chinchore, Y., A. Mitra, and P.J. Dolph. 2009. Accumulation of rhodopsin in late endosomes triggers photoreceptor cell degeneration. *PLoS Genet.* 5:e1000377. doi:10.1371/journal.pgen.1000377

Chintala, S., E.K. Novak, J.A. Spernyak, R. Mazurchuk, G. Torres, S. Patel, K. Busch, B.A. Meeder, J.M. Horowitz, M.M. Vaughan, and R.T. Swank. 2009. The Vps33a gene regulates behavior and cerebellar Purkinje cell number. *Brain Res.* 1266:18–28. doi:10.1016/j.brainres.2009.02.035

Cullinane, A.R., A. Straatman-Iwanowska, A. Zaucker, Y. Wakabayashi, C.K. Bruce, G. Luo, F. Rahman, F. Gürakan, E. Utine, T.B. Ozkan, et al. 2010. Mutations in VIPAR cause an arthrogryposis, renal dysfunction and cholestasis syndrome phenotype with defects in epithelial polarization. *Nat. Genet.* 42:303–312. doi:10.1038/ng.538

Cuttell, L., A. Vaughan, E. Silva, C.J. Escaron, M. Lavine, E. Van Goethem, J.P. Eid, M. Quirin, and N.C. Franc. 2008. Undertaker, a *Drosophila* Junctophilin, links Draper-mediated phagocytosis and calcium homeostasis. *Cell.* 135:524–534. doi:10.1016/j.cell.2008.08.033

Desjardins, M., L.A. Huber, R.G. Parton, and G. Griffiths. 1994. Biogenesis of phagolysosomes proceeds through a sequential series of interactions with the endocytic apparatus. *J. Cell Biol.* 124:677–688. doi:10.1083/jcb.124.5.677

Flannagan, R.S., G. Cosío, and S. Grinstein. 2009. Antimicrobial mechanisms of phagocytes and bacterial evasion strategies. *Nat. Rev. Microbiol.* 7:355–366. doi:10.1038/nrmicro2128

Gissen, P., C.A. Johnson, N.V. Morgan, J.M. Stapelbroek, T. Forshew, W.N. Cooper, P.J. McKiernan, L.W. Klomp, A.A. Morris, J.E. Wraith, et al. 2004. Mutations in VPS33B, encoding a regulator of SNARE-dependent membrane fusion, cause arthrogryposis-renal dysfunction-cholestasis (ARC) syndrome. *Nat. Genet.* 36:400–404. doi:10.1038/ng1325

Gissen, P., L. Tee, C.A. Johnson, E. Genin, A. Caliebe, D. Chitayat, C. Clericuzio, J. Denecke, M. Di Rocco, B. Fischler, et al. 2006. Clinical and molecular genetic features of ARC syndrome. *Hum. Genet.* 120:396–409. doi:10.1007/s00439-006-0232-z

Gong, W.J., and K.G. Golic. 2003. Ends-out, or replacement, gene targeting in *Drosophila*. *Proc. Natl. Acad. Sci. USA.* 100:2556–2561. doi:10.1073/pnas.0535280100

Harrison, R.E., C. Bucci, O.V. Vieira, T.A. Schroer, and S. Grinstein. 2003. Phagosomes fuse with late endosomes and/or lysosomes by extension of membrane protrusions along microtubules: role of Rab7 and RILP. *Mol. Cell. Biol.* 23:6494–6506. doi:10.1128/MCB.23.18.6494-6506.2003

Hershkovitz, D., H. Mandel, A. Ishida-Yamamoto, I. Chefetz, B. Hino, A. Luder, M. Indelman, R. Bergman, and E. Sprecher. 2008. Defective lamellar granule secretion in arthrogryposis, renal dysfunction, and cholestasis syndrome caused by a mutation in VPS33B. *Arch. Dermatol.* 144:334–340. doi:10.1001/archderm.144.3.334

Hoffmann, J.A. 2003. The immune response of *Drosophila*. *Nature*. 426:33–38. doi:10.1038/nature02021

Jang, J.Y., K.M. Kim, G.H. Kim, E. Yu, J.J. Lee, Y.S. Park, and H.W. Yoo. 2009. Clinical characteristics and VPS33B mutations in patients with ARC syndrome. *J. Pediatr. Gastroenterol. Nutr.* 48:348–354. doi:10.1097/MPG.0b013e31817fcb3f

Kinchen, J.M., and K.S. Ravichandran. 2008. Phagosome maturation: going through the acid test. *Nat. Rev. Mol. Cell Biol.* 9:781–795. doi:10.1038/nrm2515

Kinchen, J.M., and K.S. Ravichandran. 2010. Identification of two evolutionarily conserved genes regulating processing of engulfed apoptotic cells. *Nature*. 464:778–782. doi:10.1038/nature08853

Kinchen, J.M., K. Doukoumetzidis, J. Almendinger, L. Stergiou, A. Tosello-Trampont, C.D. Sifri, M.O. Hengartner, and K.S. Ravichandran. 2008. A pathway for phagosome maturation during engulfment of apoptotic cells. *Nat. Cell Biol.* 10:556–566. doi:10.1038/ncb1718

Kocks, C., J.H. Cho, N. Nehme, J. Ulvila, A.M. Pearson, M. Meister, C. Strom, S.L. Conto, C. Hetru, L.M. Stuart, et al. 2005. Eater, a transmembrane protein mediating phagocytosis of bacterial pathogens in *Drosophila*. *Cell.* 123:335–346. doi:10.1016/j.cell.2005.08.034

Lindmo, K., A. Simonsen, A. Brech, K. Finley, T.E. Rusten, and H. Stenmark. 2006. A dual function for Deep orange in programmed autophagy in the *Drosophila melanogaster* fat body. *Exp. Cell Res.* 312:2018–2027. doi:10.1016/j.yexcr.2006.03.002

Lo, B., L. Li, P. Gissen, H. Christensen, P.J. McKiernan, C. Ye, M. Abdelhaleem, J.A. Hayes, M.D. Williams, D. Chitayat, and W.H. Kahr. 2005. Requirement of VPS33B, a member of the Sec1/Munc18 protein family, in megakaryocyte and platelet alpha-granule biogenesis. *Blood.* 106:4159–4166. doi:10.1182/blood-2005-04-1356

Lu, H., and D. Bilder. 2005. Endocytic control of epithelial polarity and proliferation in *Drosophila*. *Nat. Cell Biol.* 7:1232–1239. doi:10.1038/ncb1324

Maldonado, E., F. Hernandez, C. Lozano, M.E. Castro, and R.E. Navarro. 2006. The zebrafish mutant vps18 as a model for vesicle-traffic related hypopigmentation diseases. *Pigment Cell Res.* 19:315–326. doi:10.1111/j.1600-0749.2006.00320.x

Matthews, R.P., N. Plumb-Rudewiez, K. Lorent, P. Gissen, C.A. Johnson, F. Lemaigre, and M. Pack. 2005. Zebrafish vps33b, an ortholog of the gene responsible for human arthrogryposis-renal dysfunction-cholestasis syndrome, regulates biliary development downstream of the onecut transcription factor hnf6. *Development.* 132:5295–5306. doi:10.1242/dev.02140

Nickerson, D.P., C.L. Brett, and A.J. Merz. 2009. Vps-C complexes: gatekeepers of endolysosomal traffic. *Curr. Opin. Cell Biol.* 21:543–551. doi:10.1016/j.ceb.2009.05.007

Pearson, A.M., K. Baksa, M. Rämet, M. Protas, M. McKee, D. Brown, and R.A. Ezekowitz. 2003. Identification of cytoskeletal regulatory proteins required for efficient phagocytosis in *Drosophila*. *Microbes Infect.* 5:815–824. doi:10.1016/S1286-4579(03)00157-6

Pevsner, J., S.C. Hsu, P.S. Hyde, and R.H. Scheller. 1996. Mammalian homologues of yeast vacuolar protein sorting (vps) genes implicated in Golgi-to-lysosome trafficking. *Gene*. 183:7–14. doi:10.1016/S0378-1119(96)00367-8

Philips, J.A., M.C. Porto, H. Wang, E.J. Rubin, and N. Perrimon. 2008. ESCRT factors restrict mycobacterial growth. *Proc. Natl. Acad. Sci. USA.* 105:3070–3075. doi:10.1073/pnas.0707206105

Poteryaev, D., S. Datta, K. Ackema, M. Zerial, and A. Spang. 2010. Identification of the switch in early-to-late endosome transition. *Cell.* 141:497–508. doi:10.1016/j.cell.2010.03.011

Pulipparacharuvil, S., M.A. Akbar, S. Ray, E.A. Sevrioukov, A.S. Haberman, J. Rohrer, and H. Krämer. 2005. *Drosophila* Vps16A is required for trafficking to lysosomes and biogenesis of pigment granules. *J. Cell Sci.* 118:3663–3673. doi:10.1242/jcs.02502

Rink, J., E. Ghigo, Y. Kalaidzidis, and M. Zerial. 2005. Rab conversion as a mechanism of progression from early to late endosomes. *Cell.* 122:735–749. doi:10.1016/j.cell.2005.06.043

Rojo, E., C.S. Gillmor, V. Kovaleva, C.R. Somerville, and N.V. Raikhel. 2001. VACUOLELESS1 is an essential gene required for vacuole formation and morphogenesis in *Arabidopsis*. *Dev. Cell.* 1:303–310. doi:10.1016/S1534-5807(01)00024-7

Sadler, K.C., A. Amsterdam, C. Soroka, J. Boyer, and N. Hopkins. 2005. A genetic screen in zebrafish identifies the mutants vps18, nf2 and foie gras as models of liver disease. *Development.* 132:3561–3572. doi:10.1242/dev.01918

Sato, T.K., P. Rehling, M.R. Peterson, and S.D. Emr. 2000. Class C Vps protein complex regulates vacuolar SNARE pairing and is required for vesicle docking/fusion. *Mol. Cell.* 6:661–671. doi:10.1016/S1097-2765(00)00064-2

Schneider, D.S., J.S. Ayres, S.M. Brandt, A. Costa, M.S. Dionne, M.D. Gordon, E.M. Mabery, M.G. Moule, L.N. Pham, and M.M. Shirasu-Hiza. 2007. *Drosophila* eiger mutants are sensitive to extracellular pathogens. *PLoS Pathog.* 3:e41. doi:10.1371/journal.ppat.0030041

Seals, D.F., G. Eitzen, N. Margolis, W.T. Wickner, and A. Price. 2000. A Ypt/Rab effector complex containing the Sec1 homolog Vps33p is required for homotypic vacuole fusion. *Proc. Natl. Acad. Sci. USA.* 97:9402–9407. doi:10.1073/pnas.97.17.9402

Sevrioukov, E.A., J.P. He, N. Moghrabi, A. Sunio, and H. Krämer. 1999. A role for the *deep orange* and *carnation* eye color genes in lysosomal delivery in *Drosophila*. *Mol. Cell.* 4:479–486. doi:10.1016/S1097-2765(00)80199-9

Smith, A.C., W.D. Heo, V. Braun, X. Jiang, C. Macrae, J.E. Casanova, M.A. Scidmore, S. Grinstein, T. Meyer, and J.H. Brumell. 2007. A network of Rab GTPases controls phagosome maturation and is modulated by *Salmonella enterica* serovar Typhimurium. *J. Cell Biol.* 176:263–268. doi:10.1083/jcb.200611056

Sriram, V., K.S. Krishnan, and S. Mayor. 2003. deep-orange and carnation define distinct stages in late endosomal biogenesis in *Drosophila melanogaster*. *J. Cell Biol.* 161:593–607. doi:10.1083/jcb.200210166

Stenmark, H., G. Vitale, O. Ullrich, and M. Zerial. 1995. Rabaptin-5 is a direct effector of the small GTPase Rab5 in endocytic membrane fusion. *Cell.* 83:423–432. doi:10.1016/0092-8674(95)90120-5

Sunio, A., A.B. Metcalf, and H. Krämer. 1999. Genetic dissection of endocytic trafficking in *Drosophila* using a horseradish peroxidase-bride of sevenless chimera: hook is required for normal maturation of multivesicular endosomes. *Mol. Biol. Cell.* 10:847–859.

Suzuki, T., N. Oiso, R. Gautam, E.K. Novak, J.J. Panthier, P.G. Suprabha, T. Vida, R.T. Swank, and R.A. Spritz. 2003. The mouse organellar biogenesis mutant buff results from a mutation in Vps33a, a homologue of yeast vps33 and *Drosophila* carnation. *Proc. Natl. Acad. Sci. USA.* 100:1146–1150. doi:10.1073/pnas.0237292100

Tanaka, T., and A. Nakamura. 2008. The endocytic pathway acts downstream of Oskar in *Drosophila* germ plasm assembly. *Development.* 135:1107–1117. doi:10.1242/dev.017293

Vergne, I., P. Constant, and G. Lanéelle. 1998. Phagosomal pH determination by dual fluorescence flow cytometry. *Anal. Biochem.* 255:127–132. doi:10.1006/abio.1997.2466

Vieira, O.V., R.J. Botelho, and S. Grinstein. 2002. Phagosome maturation: aging gracefully. *Biochem. J.* 366:689–704.

Vieira, O.V., C. Bucci, R.E. Harrison, W.S. Trimble, L. Lanzetti, J. Gruenberg, A.D. Schreiber, P.D. Stahl, and S. Grinstein. 2003. Modulation of Rab5 and Rab7 recruitment to phagosomes by phosphatidylinositol 3-kinase. *Mol. Cell. Biol.* 23:2501–2514. doi:10.1128/MCB.23.7.2501-2514.2003

Wickner, W. 2010. Membrane fusion: five lipids, four SNAREs, three chaperones, two nucleotides, and a Rab, all dancing in a ring on yeast vacuoles. *Annu. Rev. Cell Dev. Biol.* 26:115–136. doi:10.1146/annurev-cellbio-100109-104131

Zhu, G.D., G. Salazar, S.A. Zlatic, B. Fiza, M.M. Doucette, C.J. Heilman, A.I. Levey, V. Faundez, and S.W. L'hernault. 2009. SPE-39 family proteins interact with the HOPS complex and function in lysosomal delivery. *Mol. Biol. Cell.* 20:1223–1240. doi:10.1091/mbc.E08-07-0728

Akbar et al., http://www.jcb.org/cgi/content/full/jcb.201008119/DC1

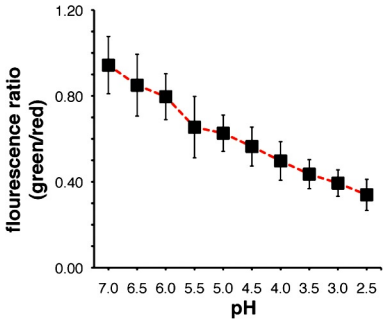

Figure S1. **Fluorescence ratio of Oregon green/Rhodamine double-labeled bacteria changes with pH.** A calibration curve was obtained from fluorescence ratios measured while incubating bacteria in defined pH buffers.

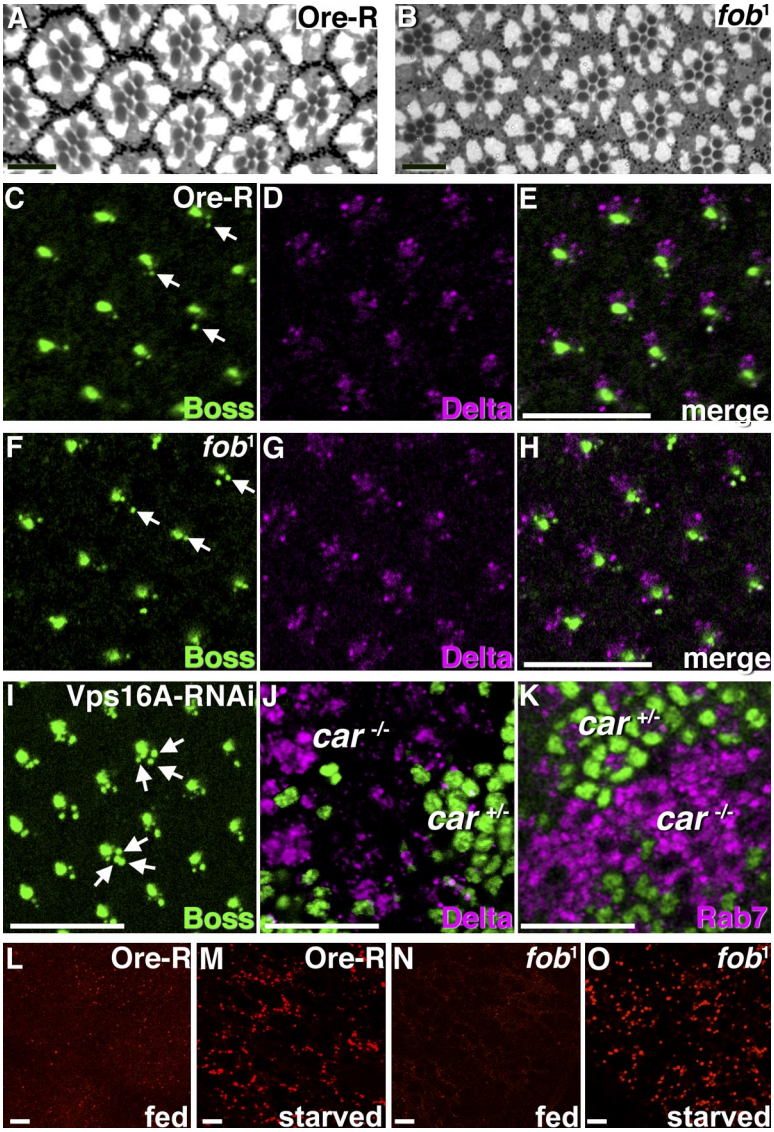

Figure S2. **Endocytic trafficking and autophagy are not altered in *fob*[1] mutants.** (A and B) Semithin sections of compound eyes from 2-d-old *fob*[1] flies (B) reveal normal arrangement of ommatidia compared with wild type (A). Ommatidial arrangement depends on normal Notch and EGF receptor signaling, which is sensitive to changes in endocytosis. (C–K) Micrographs of eye imaginal discs from larvae with the following genotypes: wild type (C–E), *fob*[1] (F–H), DA-Gal4/Vps16A-RNAi (I), FRT19-nGFP/FRT19 car$^{\Delta 146}$; Hs-Flp (J), or FRT19-nGFP/FRT19 car$^{\Delta 146}$; Hs-Flp; tub>Rab7-YFP (K). Eye discs were stained for Boss (C, F, and I) or Delta (D, G, and J). Boss is expressed on R8 cells and endocytosed into R7 cells (arrows) during signaling. Similarly, Delta is dynamically endocytosed in many cells in the developing eye disc. Neither of these ligands exhibited any significant difference between wild-type and *fob*[1] mutant tissues, but accumulated in vps16A knockdown (I) or car$^{\Delta 146}$-null cells (J). (L–O) LysoTracker staining of fat bodies was used to test induction of autophagy. No difference in autolysosomes visualized by LysoTracker was observed when comparing wild-type (L and M) and *fob*[1] mutant (N and O) fat bodies before (L and N) or after (M and O) 4 h of protein starvation. Bars, 10 µm.

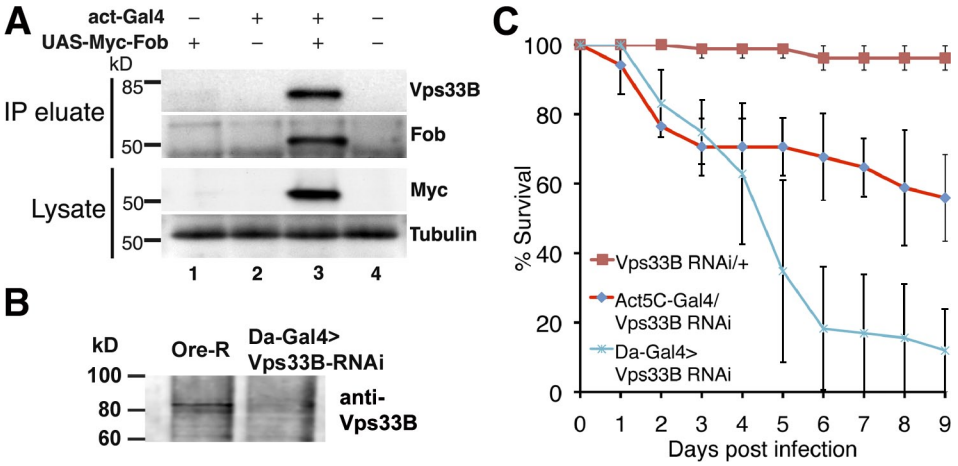

Figure S3. **Vps33B binds Fob in vivo and is necessary for normal immune defense.** (A) Myc-Fob was expressed under Act-Gal4 control in *fob*^{1} background and immunoprecipitated using anti-Myc antibody. Expression of Myc-Fob was detected in whole fly lysates. Tubulin was used as loading control. Myc-Fob coimmunoprecipitated endogenous dVps33B, as detected in immunoprecipitated eluates with anti-Vps33B antibodies raised against a dVps33B-His6 fusion protein. UAS-Myc-Fob only (lane 1), Act-Gal4 only (lane 2), and *fob*^{1} (lane 4) without transgenes were used as experimental controls. The genotypes used were: w/w; uas-Myc-Fob/+; +/+ (lane 1), w/w; Act-Gal4/+; +/+ (lane 2), w/w; Act-Gal4/uas-Myc-Fob; *fob*^{1}/*fob*^{1} (lane 3), and w/w; +/+; *fob*^{1}/*fob*^{1} (lane 4). (B) Da-Gal4/Vps33B-RNAi flies exhibited reduced levels of Vps33B compared with wild type (Ore-R). Before detection on Western blots, lysates were enriched for Vps33B by immunoprecipitation with anti-Vps33B-beads. (C) Survival after infection with *E. coli* was measured for flies with uas-Vps33B RNAi expressed under the control of one copy of Actin5C-Gal4, two copies of Da-Gal4, or no driver. Although two copies of Da-Gal4 were more efficient, expression with either driver caused *E. coli*–infected flies to die significantly faster when compared with control with no Gal4 driver ($P < 0.001$, logrank). Importantly, like *fob*^{1}, flies homozygous for Da-Gal4 and uas-Vps33B-RNAi were homozygous viable and fertile, and lacked any overt developmental defects. Error bars represent mean values with standard deviation.